ELSEVIER

Thermochimica Acta 274 (1996) 261–272

thermochimica acta

Thermal decomposition of rare-earth-doped calcium oxalate. Part 1. Doping with lanthanum, samarium and gadolinium

Usharani Patnaik, J. Muralidhar *

CPAF Division, Regional Research Laboratory, Bhubaneswar-751 013, Orissa, India

Received 28 December 1994; accepted 31 March 1995

Abstract

The thermal decomposition of calcium oxalate doped with lanthanum, samarium or gadolinium has been investigated using thermogravimetry (TG) and differential thermal analysis (DTA). The kinetics of the decomposition steps have been studied by the non-isothermal TG technique. The doped oxalates decompose in a similar way to pure CaOx. After dehydration, decomposition of doped oxalates proceeds in two overlapping exothermic stages, i.e. decomposition of lanthanide oxalates followed by that of calcium oxalate. Samples heated up to 1000°C reveal the existence of CaO and Ln_2O_3 in separate phases.

Keywords: Decomposition; Doping; Gadolinium; Lanthanum; Samarium

1. Introduction

Thermal decomposition studies of oxalates are of importance in synthesizing superconducting double or multicomponent oxides [1,2]. High purity titanates, stannates, ferrites, and zirconates of perfect stoichiometry can be prepared from mixed metal oxalate systems [3,5]. Decomposition of alkaline earth (Ca, Sr and Ba) copper oxalate compounds at high temperature leads to the formation of high purity $MCuO_2$ [6]. Thermal studies of lanthanide oxalates prepared either by mechanical mixing or by co-precipitation methods have been reported by various workers [7,10]. Calcium oxalate is used as an effective carrier for separation of small quantities of rare earth elements from the ore by co-precipitation methods [11]. In the present investigation,

* Corresponding author.

SSDI 0040-6031(95)02394-1

calcium oxalate was doped with lanthanum, samarium and gadolinium, and their thermal decomposition behaviours studied.

2. Experimental

All the chemicals used were of analytical grade, unless otherwise specified.

2.1. Preparation of oxalates

Calcium oxalate monohydrate was prepared by precipitation using the homogeneous solution method [12]. Oxides of lanthanum, samarium and gadolinium (Goodfellow, UK) were dissolved in dilute nitric acid. Corresponding oxalate decahydrates were precipitated from the nitrate solution as reported by Wendlandt [13].

2.2. Synthesis of coprecipitated calcium–lanthanide oxalates

Calculated amounts of calcium carbonate and lanthanide nitrate solutions required for different mixed oxalate compositions were dissolved together in dilute nitric acid. The oxalates were then precipitated from the hot solution by adding 5% (w/v) ammonium oxalate solution. The pH of the solution was controlled within 6–6.5 by the addition of dilute ammonium hydroxide solution. The solution was digested on a hot water bath for 2 h for fine crystal formation. The precipitate was then filtered, washed with distilled water and dried under suction for 3 h. Compositional analyses of these coprecipitated oxalates were carried out by conventional chemical methods [14,15]. The number of water molecules in the oxalates were determined from the weight loss in the dehydration step, as described by El-Houte and El-Sayed Ali [9].

The coprecipitated oxalates have the general formula $Ca_{2-x}Ln_x(C_2O_4)_{2+x/2}\cdot 2H_2O$, where x is the mole fraction of lanthanide. Results of the compositional analysis are presented in Table 1.

2.3. Instrumental

Simultaneous TG-DTA data were recorded with a linear heating rate of 10°C min^{-1} under static air on a Shimadzu DT-40 thermal analyser. Open alumina crucibles of identical dimensions were used with α-Al_2O_3 as the DTA reference material. The samples (10 mg) were pyrolysed up to 1000°C.

X-ray powder diffraction data of the samples were obtained using a Philips PW 1710 X-ray diffractometer with a nickel filter and Cu K_α radiation.

3. Results and discussion

Calcium oxalate monohydrate has the following three basic decomposition steps

$$CaC_2O_4\cdot H_2O \rightarrow CaC_2O_4 + H_2O \quad (1)$$

Table 1
Compositional analysis of coprecipitated oxalates

Wt% La^{3+}	Oxalate identification	Ca Theor. (Obs.) %	Ln Theor. (Obs.) %	C_2O_4 Theor. (Obs.) %	H_2O (Theor. Obs.) %
1% La	$Ca_{1.96}La_{0.04}Ox_{2.02}\cdot 2H_2O$	26.31 (26.91)	1.91 1.85	59.68 (61.47)	12.0 (10.0)
5% La	$Ca_{1.82}La_{0.18}Ox_{2.18}Ox_{2.09}\cdot 2H_2O$	22.87 (23.13)	7.95 7.72	57.85 (58.15)	11.0 (11.3)
10% La	$Ca_{1.68}La_{0.32}Ox_{2.16}\cdot 2H_2O$	19.89 (22.62)	13.16 12.90	56.28 (56.41)	10.3 (10.6)
1% Sm	$Ca_{1.96}Sm_{0.04}Ox_{0.02}\cdot 2H_2O$	26.22 (25.2)	2.15 2.00	59.58 (59.80)	11.9 (12.0)
5% Sm	$Ca_{1.81}Sm_{0.19}Ox_{2.09}\cdot 2H_2O$	22.56 (23.06)	8.80 8.70	57.41 (57.99)	10.9 (11.0)
10% Sm	$Ca_{1.67}Sm_{0.33}Ox_{2.16}\cdot 2H_2O$	19.50 (19.80)	14.43 14.35	55.56 (56.10)	9.9 (10.0)
1% Gd	$Ca_{1.96}Gd_{0.04}Ox_{2.02}\cdot 2H_2O$	26.17 (26.45)	2.29 2.05	59.49 (60.32)	11.9 (9.0)
5% Gd	$Ca_{1.81}Gd_{0.19}Ox_{2.09}\cdot 2H_2O$	22.39 (23.21)	9.34 9.50	57.11 (57.78)	10.8 (11.2)
10% Gd	$Ca_{1.67}Gd_{0.33}Ox_{2.17}\cdot 2H_2O$	19.26 (19.50)	15.18 15.25	55.14 (54.90)	9.8 (9.5)

$$CaC_2O_4 \rightarrow CaCO_3 + CO \quad (2a)$$

$$CO + 0.5O_2 \rightarrow CO_2 \quad (2b)$$

$$CaCO_3 \rightarrow CaO + CO_2 \quad (3)$$

Reactions (1) and (3) give endothermic DTA peaks. Reaction (2) which usually gives an endothermic DTA peak in an inert atmosphere, shows an exothermic DTA peak in static air due to the catalytic effect of the $CaCO_3$ formed in reaction (2a) on the exothermic reaction (2b) [16].

Figs. 1–4 show the simultaneous TG-DTA results obtained on both pure oxalates and the coprecipitated oxalates in static air. All the samples studied exhibit similar thermal decomposition patterns to that of pure calcium oxalate. However, the baseline drift observed in the case of the oxalates doped with gadolinium indicates the high ionic conductivity of the sample. The decomposition of these oxalates can be studied in detail under three headings, namely dehydration, decomposition of oxalate to carbonate, and decomposition of carbonate to oxide. The kinetics of these decomposition steps have been studied by non-isothermal methods using experimental data obtained from thermogravimetric curves. Conversion functions of the type $f(\alpha)=(1-\alpha)^n$, with $n=0$, 1/2, 1/3, 2/3, 1 and 2, have been used for the reaction mechanism identification. The most suitable reaction mechanism was chosen by the best fitting straight line with the highest square of the correlation coefficient (r^2) from the $\ln(g(\alpha)/T^2)$ vs. $1/T$ plot.

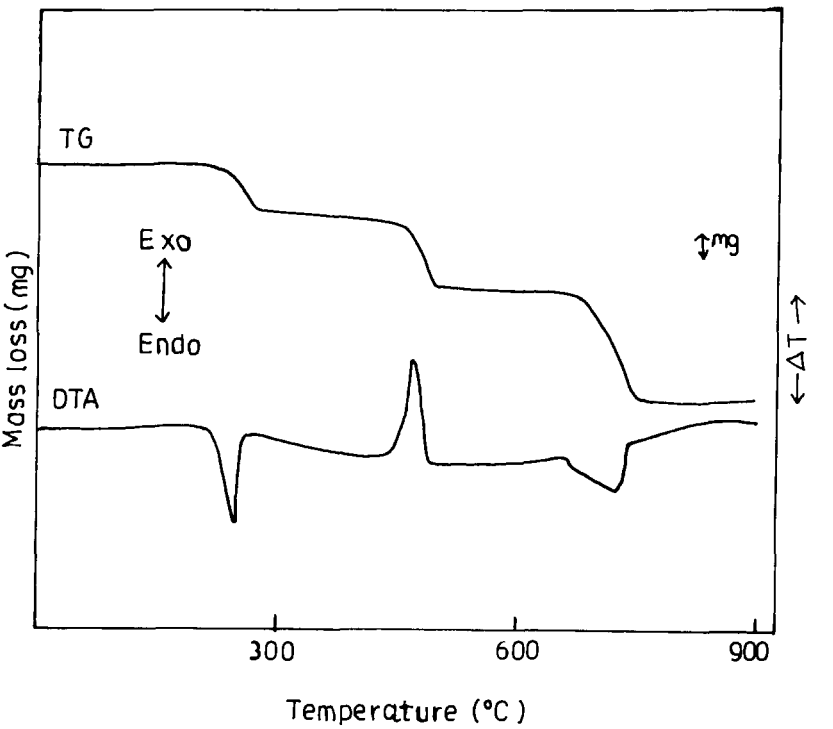

Fig. 1. Simultaneous TG-DTA curve of pure $CaOx{\cdot}H_2O$. 10 mg sample, static air, rate of heating, $10°C\,min^{-1}$.

Kinetic parameters such as the activation energy (E) and frequency factor (A) were determined using the Coats–Redfern equation [17].

3.1. Dehydration of oxalates

The coprecipitated oxalates exhibit only one endothermic DTA peak in the region 130–200°C. The weight loss from the TG trace in this region corresponds to the loss of two molecules of water of crystallisation. Table 2 gives a comparison of the experimental weight losses with the theoretical weight losses in the dehydration and decomposition steps of all these oxalates.

Interestingly, the XRD patterns of coprecipitated oxalate hydrates do not exhibit peaks corresponding to lanthanide oxalates but peaks with slight distortions from those of $CaC_2O_4{\cdot}H_2O$. This indicates the presence of a homogeneous phase which loses two water molecules in a single step on heating to 200°C.

Table 3 lists the activation energies and pre-exponential factors (as $\ln(A/s^{-1})$, together with $g(\alpha)$ and r^2 values estimated for the dehydration step of the coprecipitated oxalates. Dehydration follows a first-order mechanism (F_1), governed by the conversion integral $g(\alpha = -\ln(1-\alpha)$. The activation energy decreases as the concentration of a particular dopant increases.

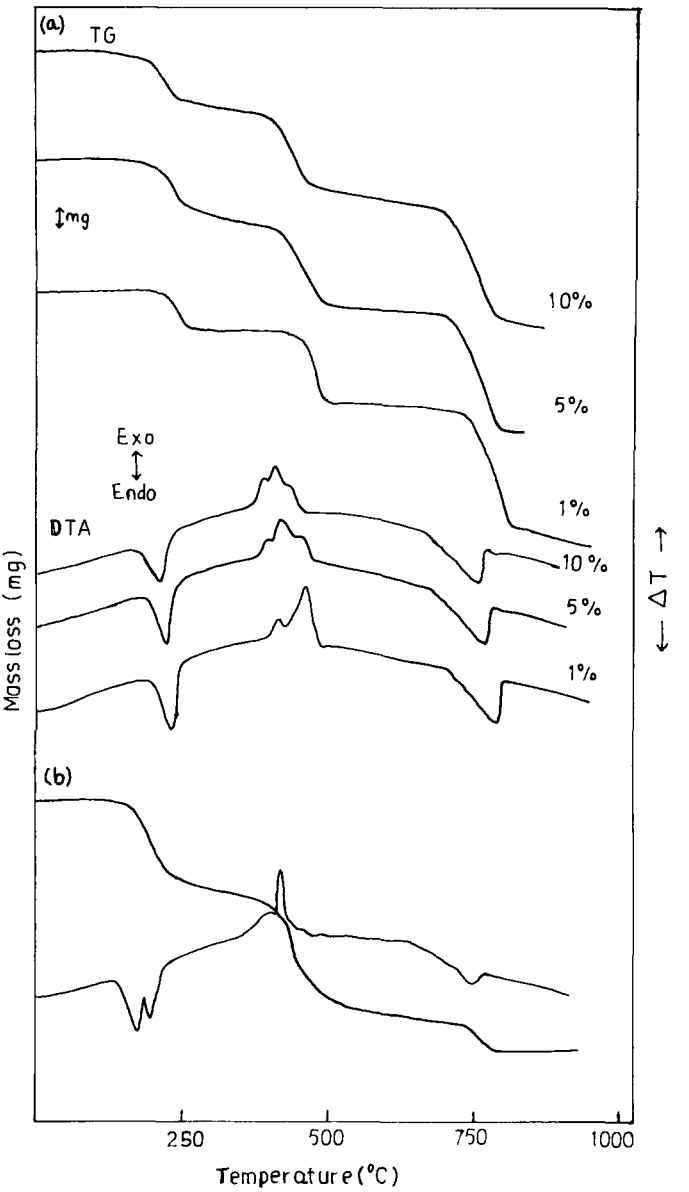

Fig. 2. Simultaneous TG-DTA curve of: (a) CaOx doped with 1%, 5% and 10% La; (b) pure $La_2(C_2O_4)_3 \cdot 10H_2O$. 15 mg sample, static air, rate of heating, 10°C min^{-1}.

3.2. *Decomposition of anhydrous oxalates*

Decomposition of anhydrous CaOx occurs within the 415–490°C region with an exothermic DTA peak in static air. However, for the anhydrous coprecipitated oxalates

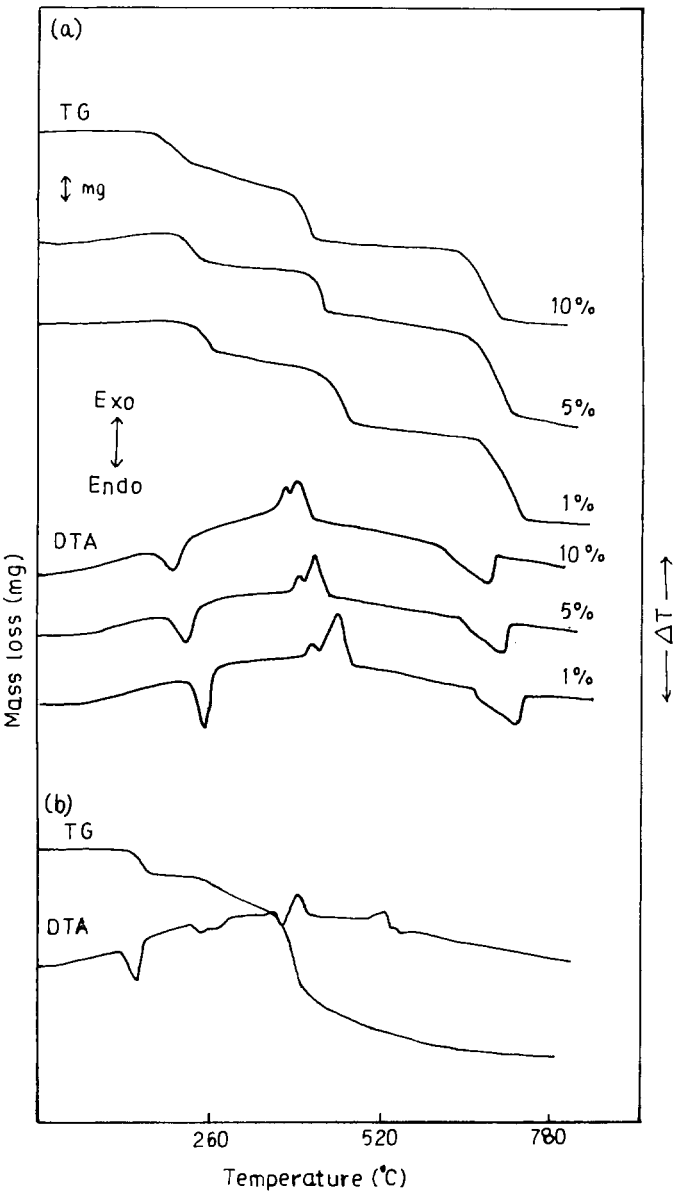

Fig. 3. Simultaneous TG-DTA curve of: (a) CaOx doped with 1%, 5% and 10% Sm; (b) pure $Sm_2(C_2O_4)_3 \cdot 10H_2O$. 10 mg sample, static air, rate of heating, 10°C min^{-1}.

with samarium or gadolinium, the exotherm spilts into two. The first small exotherm becomes more and more dominant with the increase in dopant concentration. The splitting may indicate either the formation of an intermediate during decomposition or the occurrence of decomposition in two separate steps. The latter is more likely because

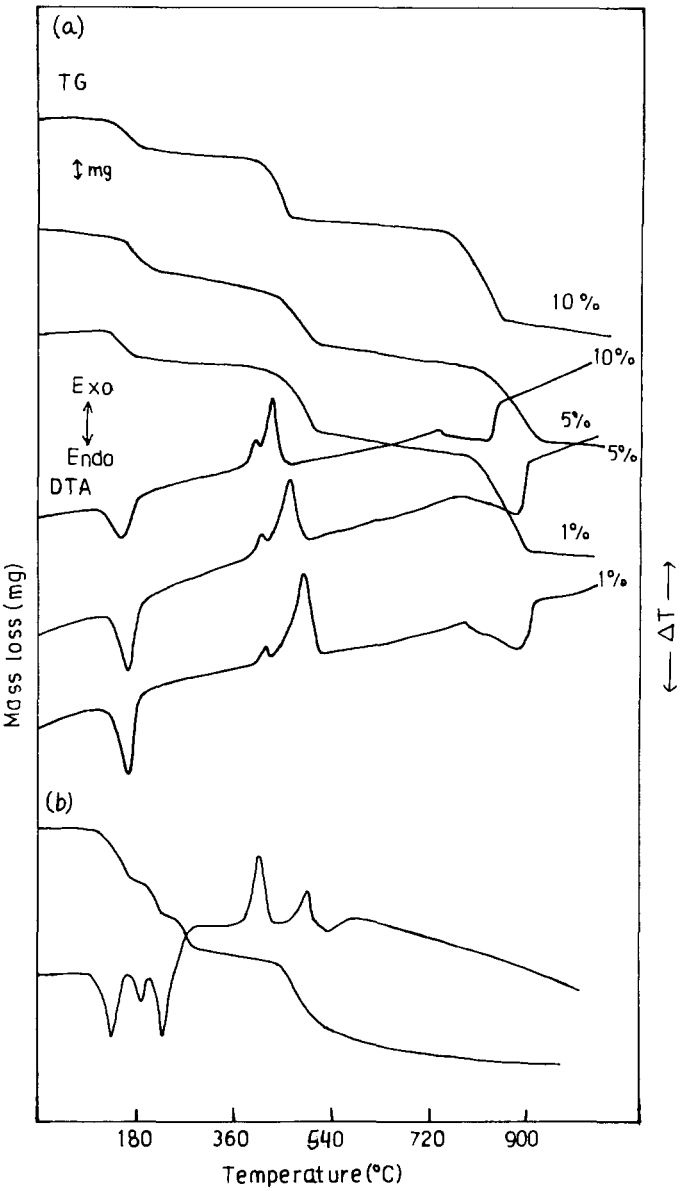

Fig. 4. Simultaneous TG-DTA curve of: (a) CaOx doped with 1%, 5% and 10% Gd; (b) pure $Gd_2(C_2O_4)_3 \cdot 10H_2O$. 10 mg sample, static air, rate of heating, 10°C min^{-1}.

the first small exotherm occurs at around the peak decomposition temperature of lanthanide oxalate (370°C) and the second large exotherm occurs at about the decomposition temperature of CaOx (460°C). Further evidence can be obtained from XRD data on the dehydrated coprecipitated oxalates. The data (Table 4) reveal the

Table 2
Thermoanalytical data on coprecipitated oxalate hydrates

Oxalate composition	Dehydration			Oxalate decomp.			Carbonate decomp.		
	Temp./°C	% Wt. loss		Temp./°C	% Wt. loss		Temp./°C	% Wt. loss	
		calc.	obs.		calc.	obs.		calc.	obs.
$CaOx \cdot H_2O$	180	12.3	12.5	460	21.9	22.8	775	44.0	45.2
CaOx + 1% La	175	12.0	10.0	375, 423	21.7	21.2	783	43.3	43.6
CaOx + 5% La	180	11.0	11.3	365, 395, 440	21.3	23.2	793	40.8	40.9
CaOx + 10% La	175	10.3	10.6	365, 393, 443	20.9	21.5	775	38.2	38.5
CaOx + 1% Sm	175	11.9	12.0	372. 425	21.6	24.9	765	43.2	43.5
CaOx + 5% Sm	163	10.9	11.0	372, 402	21.2	21.3	760	40.7	42.0
CaOx + 10% Sm	170	9.9	10.0	377, 400	21.1	22.2	765	38.0	38.0
CaOx + 1% Gd	187	11.9	9.0	389, 451	21.4	22.6	776	43.3	45.1
CaOx + 5% Gd	195	10.8	11.2	393, 437	21.2	22.6	775	40.7	41.6
CaOx + 10% Gd	181	9.8	9.5	402, 428	21.0	21.6	783	38.1	39.3

Temperatures reported are the peak decomposition temperatures.

Table 3
Kinetic parameters with appropriate $g(\alpha)$ for dehydration of coprecipitated oxalate hydrates

Oxalate composition	$g(\alpha)$	E/(kJ mol^{-1})	ln(A/s^{-1})	r^2
$CaOx \cdot H_2O$		144.1	47	0.9816
CaOx + 1% La		107.7	23	0.9931
CaOx + 5% La		96.2	18	0.9598
CaOx + 10% La		87.2	17	0.9623
CaOx + 1% Sm	F_1	141.1	46	0.9814
CaOx + 5% Sm		109.6	24	0.9920
CaOx + 10% Sm		72.8	12	0.9746
CaOx + 1% Gd		122.8	27	0.9889
CaOx + 5% Gd		116.2	25	0.9789
CaOx + 10% Gd		88.2	18	0.9903

Table 4
XRD data of coprecipitated oxalates after heating to 200°C

Oxalate composition	d	Oxalate composition	d	Oxalate composition	d
CaOx + 10% La	3.657	CaOx + 10% Sm	3.688	CaOx + 10% Gd	3.667
	2.984		2.994		2.979
	2.910		2.881		2.906
	1.846		1.833		1.856
	3.101		3.699		3.332
	2.986		3.333		2.267
	2.881		2.792		2.086
	2.612		1.817		1.856

The first four d-values are for α-CaOx, and last are for the corresponding anhydrous lanthanide oxalates.

presence of prominent lanthanide oxalate peaks along with those of CaOx. Therefore, after dehydration, the component oxalates retain their individuality in the coprecipitated oxalates.

In coprecipitates of CaOx and lanthanum oxalate, the single exotherm splits into three peaks. Glasner and Steinberg [18] who worked on the thermal decomposition of lanthanum oxalate, also observed a two-stage decomposition during the oxalate breakdown step. They observed an intermediate of composition $La_2C_2O_4(CO_3)_2$ during the first stage of decomposition and a subsequent exothermic peak for the total decomposition of the oxalate complex to $La_2(CO_3)_3$. In the present investigation, the first exotherm at 365°C is due to the decomposition of lanthanum oxalate to the intermediate A, of composition $La_2(C_2O_4)(CO_3)_2$; the second exotherm at 395°C is due to the decomposition of intermediate A to $La_2(CO_3)_3$, and the third exotherm at 440°C corresponds to the decomposition of CaOx. A comparison of the peak decomposition temperatures for all the coprecipitated oxalates reveals that their thermal stabilities are less than that of pure CaOx and decrease with the increase in lanthanide concentration.

The lowering of the decomposition temperature of doped CaOx is caused by the earlier initiation of the exothermic decomposition of the lanthanide oxalates contained in it. Since oxalate breakdown begins very slowly, overlaps between the decompositions of lanthanide oxalate and CaOx cannot be discounted.

Even though the DTA curves show a split in the exothermic peak, the corresponding TG curves show only a continuous weight loss within the region 360–475°C. Furthermore, decomposition of calcium oxalate starts before the completion of decomposition of lanthanide oxalate. Therefore, it is difficult to study the kinetics of individual breakdown steps. Thus, an overall kinetic study of the oxalate breakdown steps has been made. The linearity of the $\ln(g(\alpha)/T^2)$ vs. $1/T$ plot was observed within the α range 0.1–0.9. The kinetic parameters obtained for this step are presented in Table 5.

3.3. *Decomposition of carbonates*

All the carbonates formed in reaction step (2) undergo pyrolytic decomposition to the corresponding oxides in the temperature range 690–810°C. It can be seen from

Table 5
Kinetic parameters with appropriate $g(\alpha)$ for the overall oxalate breakdown step

Oxalate composition	$g(\alpha)$	E/(kJ mol^{-1})	$\ln(A/s^{-1})$	r^2
CaOx·H_2O		282.44	39	0.9993
CaOx + 1% La		219.40	31	0.9951
CaOx + 5% La		126.50	15	0.9937
CaOx + 10% La		124.40	15	0.9976
CaOx + 1% Sm	R_2	181.18	25	0.9865
CaOx + 5% Sm		181.10	25	0.9960
CaOx + 10% Sm		171.84	23	0.9944
CaOx + 1% Gd		179.66	23	0.9905
CaOx + 5% Gd		187.49	25	0.9906
CaOx + 10% Gd		210.66	29	0.9929

Table 6
Kinetic parameters with appropriate $g(\alpha)$ for the carbonate breakdown step

Oxalate composition	$g(\alpha)$	E/(kJ mol^{-1})	$\ln(A/s^{-1})$	r^2
CaOx·H_2O		201.9	15	0.9980
CaOx + 1% La		171.8	13	0.9888
CaOx + 5% La		171.3	32	0.9983
CaOx + 10% La	A_2	190.1	17	0.9814
CaOx + 1% Sm		187.5	14	0.9907
CaOx + 5% Sm		187.2	13	0.9961
CaOx + 10% Sm		188.9	13	0.9935
CaOx + 1% Gd		163.7	13	0.9985
CaOx + 5% Gd		182.8	15	0.9946
CaOx + 10% Gd		175.4	14	0.9951

Table 7
XRD data of coprecipitated oxalates after heating to 830°C for 3h

Oxalate composition	*d*	Oxalate composition	*d*	Oxalate composition	*d*
CaOx + 10% La	2.791	CaOx + 10% Sm	2.790	CaOx + 10% Gd	2.789
	2.415		2.412		2.409
	1.705		1.705		1.718
	1.454		1.452		1.441
	2.994		3.190		3.138
	2.286		2.980		2.704
	1.975		2.851		1.916
	1.750		1.931		1.635

The first four *d*-values are for CaO, and last are for the corresponding anhydrous lanthanide, oxides.

Figs. 2–4 that no separate DTA peak is observed for the lanthanide carbonate decomposition. The kinetic parameters for the carbonate decomposition steps are presented in Table 6.

The X-ray diffraction data (Table 7) of the final decomposition products (after calcination at 830°C for 3 h) from the doped oxalates with 10% lanthanides, reveal the existence of both CaO and Ln_2O_3 in separate phases. This is in agreement with the published results [19].

Acknowledgements

The authors thank the Director, R.R.L. Bhubaneswar, for permission to publish this work. One of the authors (URP) thanks C.S.I.R., New Delhi, for awarding the fellowship.

References

[1] S. Uma and J. Gopalakrishnan, J. Solid State Chem., 102(2) (1993) 332.
[2] R.K. Sinha and S.K. Srivastava, Supercond. Sci. Technol., 6(4) (1993) 238.
[3] I. Aboltina, R. Ramata and I. Brante, Ferroelectrics, 141(3–4) (1993) 277.
[4] A.K. Sharma and N.K. Kaushik, Thermochim. Acta, 83(2) (1985) 347.
[5] V.B. Reddy and P.N. Mehrotra, J. Therm. Anal., 21 (1981) 21.
[6] M. Insausti, R. Cortes, M.I. Arriortua, T. Rojo and E.H. Bocaregra, Solid State Ionics, 63–65(1–4) (1993) 351.
[7] M.J. Fuller and J. Pinkstone, J. Less Common Metals, 70(2) (1980) 127.
[8] W.W. Wendlandt, T. George and G.R. Horton, J. Inorg. Nucl. Chem., 273 (1961) 280.
[9] S. El-Houte and M. El-Sayed Ali, J. Therm. Anal., 37 (1991) 907.
[10] Y. Watanabe, S. Miyazaki, T. Maruyama and Y. Saito, Thermochim. Acta, 88 (1985) 295.
[11] B.C. Purukayastha and S.N. Bhattacharya, J. Inorg. Nucl. Chem., 10 (1959) 103.
[12] A.I. Vogel, Text Book of Quantitative Inorganic Analysis, Longmans, London, 3rd edn., 1961, p. 501.
[13] W.W. Wendlandt, Anal. Chem., 30 (1958) 58.

[14] A.I. Vogel, Text Book of Quantitative Inorganic Analysis, Longmans, London, 3rd edn., 1961, p. 282, 436.
[15] R. Pribil, Analytical Applications of EDTA and Related Compounds, Vol. 52, Pergamon Press, Oxford, 1972, p. 165.
[16] D. Dollimore and D.L. Griffiths, J. Therm. Anal., 2 (1970) 229.
[17] A.W. Coats and J.P. Redfern, Nature, 201 (1964) 68.
[18] A. Glasner and M. Steinberg, J. Inorg. Nucl. Chem., 22 (1961) 39.
[19] K.W. Bagnall (Ed.), MTP International Review of Science, Inorg. Chem., Series 1, Vol. 1, Butterworth, London, 1972, p. 78.